JOURNAL OF VIROLOGY, Nov. 2009, p. 10922–10930 Vol. 83, No. 21
0022-538X/09/$12.00 doi:10.1128/JVI.01312-09

Low pH-Triggered Beta-Propeller Switch of the Low-Density Lipoprotein Receptor Assists Rhinovirus Infection▽

Tuende Konecsni,[1] Ursula Berka,[2] Angela Pickl-Herk,[1] Gerhard Bilek,[1] Abdul Ghafoor Khan,[1] Leszek Gajdzig,[2] Renate Fuchs,[2] and Dieter Blaas[1]*

Max F. Perutz Laboratories, University Departments at the Vienna Biocenter, Department of Medical Biochemistry, Medical University of Vienna, Vienna, Austria,[1] and Department of Pathophysiology, Medical University of Vienna, Vienna, Austria[2]

Received 26 June 2009/Accepted 5 August 2009

Minor group human rhinoviruses (HRVs) bind three members of the low-density lipoprotein receptor (LDLR) family: LDLR proper, very-LDLR (VLDLR) and LDLR-related protein (LRP). Whereas ICAM-1, the receptor of major group HRVs actively contributes to viral uncoating, LDLRs are rather considered passive vehicles for cargo delivery to the low-pH environment of endosomes. Since the Tyr-Trp-Thr-Asp β-propeller domain of LDLR has been shown to be involved in the dissociation of bound LDL via intramolecular competition at low pH, we studied whether it also plays a role in HRV infection. Human cell lines deficient in LDLR family proteins are not available. Therefore, we used CHO-*ldla7* cells that lack endogenous LDLR. These were stably transfected to express either wild-type (wt) human LDLR or a mutant with a deletion of the β-propeller. When HRV2 was attached to the propeller-negative LDLR, a lower pH was required for conversion to subviral particles than when attached to wt LDLR. This indicates that high-avidity receptor binding maintains the virus in its native conformation. HRV2 internalization directed the mutant LDLR but not wt LDLR to lysosomes, resulting in reduced plasma membrane expression of propeller-negative LDLR. Infection assays using a CHO-adapted HRV2 variant showed a delay in intracellular viral conversion and de novo viral synthesis in cells expressing the truncated LDLR. Our data indicate that the β-propeller attenuates the virus-stabilizing effect of LDLR binding and thereby facilitates RNA release from endosomes, resulting in the enhancement of infection. This is a nice example of a virus exploiting high-avidity multimodule receptor binding with an intrinsic release mechanism.

Human rhinoviruses (HRVs), members of the picornavirus family of nonenveloped, single-stranded positive-sense RNA viruses, are the major cause of the common cold. Based on phylogeny, they are divided into two species, HRV-A and HRV-B. For cell entry, HRVs use two different types of receptors; 87 major group viruses bind human intercellular adhesion molecule 1 (ICAM-1) (44), while 12 types (the minor group) attach to members of the low-density lipoprotein receptor (LDLR) family, including LDLR, very-LDLR (VLDLR), and LDLR-related protein (LRP) (46). All minor group HRVs are HRV-A, but major group HRVs belong to either species. Recently, a new clade tentatively termed HRV-C was identified (23), but its properties with respect to receptor binding and entry have not been elucidated.

The minor group virus HRV2 enters via clathrin-dependent endocytosis (41). This is not unexpected since LDLRs possess a clathrin localization signal in their C-terminal cytoplasmic domains. However, when the clathrin-dependent pathway is blocked, similar to physiologic ligands, HRV2 might also exploit other endocytosis routes (3). After cell entry, HRVs of both receptor groups end up in endosomal compartments. For major group HRVs either ICAM-1 alone or in concert with the low-pH environment triggers conversion into subviral particles; concomitantly, the virion is uncoated, and the genomic RNA is released (33). In contrast, structural changes and infection of the minor group viruses exclusively depend on the low endosomal pH, and it was believed that the function of LDLRs was limited to virus delivery (8).

Exposure to pH ≤3 inactivates all HRVs, and this property was originally used as a means for their classification (43). However, most HRVs already convert into subviral particles and thereby lose infectivity at much higher pH values. For example, HRV2 readily experiences conformational modifications below a threshold pH of 5.6 in vitro and in vivo (16, 34), and inactivation occurs within a range of ~0.6 pH units according to a sigmoid progression. On the other hand, some major group viruses were found to be more stable (20).

During infection, native virus is first converted into subviral A-particles that still contain RNA but have lost the innermost capsid protein VP4. They no longer attach to their respective receptors but are hydrophobic because of externalization of the amphipathic N termini of VP1 that are believed to insert into the lipid bilayer of the endosomal membrane (28). In a next step, the RNA is transferred into the cytosol, leaving behind empty hydrophilic subviral B particles. These processes are strongly coordinated, as indicated by the in vitro membrane-disrupting activity of VP4 (11). VP4 appears to also play an essential role in RNA transfer. Furthermore, when VP0 is not cleaved into VP2 and VP4 during viral maturation, the virions bind to their receptors and undergo all structural tran-

* Corresponding author. Mailing address: Max F. Perutz Laboratories, University Departments at the Vienna Biocenter, Department of Medical Biochemistry, Medical University of Vienna, Dr. Bohr Gasse 9/3, A-1030 Vienna, Austria. Phone: 43 1 4277 61630. Fax: 43 1 4277 9616. E-mail: dieter.blaas@meduniwien.ac.at.

▽ Published ahead of print on 12 August 2009.

sitions but fail to initiate infection most probably because the RNA does not arrive in the cytosol (26).

The conformational modifications of the major group virus HRV14 result in disruption of the endosome; on the other hand, the minor group virus HRV2 opens a pore in the membrane for the RNA to enter the cytosol and the endosome remains largely intact (35, 39). In the latter case, empty particles are left and are shuttled to lysosomes for degradation. Conversely, HRV14 capsid proteins arrive, together with the viral RNA in the cytosol. Therefore, the capsid is degraded to a much lesser extent since it fails to reach the lysosomes.

C-terminal from the ligand-binding domain, LDLR possesses an epidermal growth factor (EGF)-precursor homology (EGFP) domain with two cysteine-rich EGF-like repeats (EGF-A and -B), a six-bladed β-propeller with characteristic Tyr-Trp-Thr-Asp (YWTD) motives, and a third EGF repeat (EGF-C). The three-dimensional structure of LDLR at pH 5.3 shows a closed conformation, in which ligand binding repeats L4 and L5 fold back toward the β-propeller, establishing an intramolecular interaction (37). This involves lysine and tryptophan residues similar to those conferring binding of VLDLR to HRV2 (45) and LDLR to receptor-associated protein at neutral pH (13). Moreover, a number of histidine residues in the propeller become partly protonated and establish additional ionic interactions with buried negatively charged residues of the two ligand binding repeats. This intramolecular competition for the ligand-binding repeats is believed to be responsible for the release of bound LDL at low pH. However, recent mutagenesis experiments suggest that the three histidines supposed to participate in this competition are rather involved in an allosteric mechanism lowering the affinity of the ligand for the receptor at the low endosomal pH (48).

Since virus conversion and release from the receptor is triggered by acid pH in any case, we sought to determine whether competition by the β-propeller played any role in viral infection. Comparing the behavior of wild-type (wt) and propeller-deficient LDLR in HRV2 infection, we demonstrate that the β-propeller promotes infection by facilitating virus conversion and RNA release in the appropriate endosomal compartments within a suitable time window. These results show that minor group receptors are not just passive vehicles for virus delivery but actively contribute to infection.

MATERIALS AND METHODS

Chemicals. All chemicals were obtained from Sigma (St. Louis, MO) or Merck (Darmstadt, Germany) unless specified otherwise. WIN-52084-2 (kindly provided by Dan Pevear, ViroPharma) was dissolved at 0.5 mg/ml in 50% dimethyl sulfoxide and stored at −20°C. Tissue culture plates and flasks were from Iwaki (Bibby Sterilin, Stone, Staffordshire, United Kingdom).

Buffer solutions. Isotonic 30 mM MES (morpholinoethanesulfonic acid) buffers were adjusted to a pH between 4.8 and 7.0 with 0.2 increments. To ensure isotonicity, the NaCl concentrations were calculated by using the web tool "Recipe Calculator for Thermodynamically Correct Buffers," of the University of Liverpool, (http://www.liv.ac.uk/buffers/buffercalc.html). After addition of the adequate amount of NaCl, the buffers were brought to the respective pH with NaOH at 0°C. Hanks balanced buffer solution (HBBS; 0.137 M NaCl, 5.4 mM KCl, 0.25 mM Na_2HPO_4, 0.44 mM KH_2PO_4, 1.3 mM $CaCl_2$, 1.0 mM $MgSO_4$, 4.2 mM $NaHCO_3$) was used for washes, as well as for incubation of CHO cells at 4°C as specified in the text. Radioimmunoprecipitation assay (RIPA) buffer (50 mM Tris-HCl [pH 7.5], 150 mM NaCl, 1 mM EDTA, 1% sodium deoxycholate, 0.1% sodium dodecyl sulfate, 1% Triton X-100) was used for cell lysis prior to radioimmunoprecipitation and/or scintillation counting.

Cell lines. HeLa-H1 Ohio cells (American Type Culture Collection, Manassas, VA), a subline supporting the replication of HRVs, were used for HRV2 production and labeling with [^{35}S]methionine-cysteine, as well as for titer determination. CHO-*ldla7* Chinese hamster ovary cells lacking functional endogenous LDLRs (22) but stably transfected to overexpress native human LDLR (termed RF3 cells) or LDLR in which the YWTD β-propeller domain and the EGF-C domain are deleted (termed ΔYC cells) (5, 6), kindly provided by Stephen Blacklow (Boston, MA), were used in all other experiments.

Cell culture medium. HeLa-H1 cells (for short HeLa) were cultured in minimal essential medium (MEM) supplemented with 10% heat-inactivated fetal calf serum (FCS), 2 mM L-glutamine, 100 U of penicillin/ml, and 100 μg of streptomycin/ml (Gibco/Invitrogen Corp., Paisley, United Kingdom). For infection of HeLa cells, MEM containing 30 mM $MgCl_2$ and 2% FCS (infection medium) was used. CHO cells were cultured in Ham F-12 medium with 5% FCS, 2 mM L-glutamine, 100 U of penicillin/ml, and 100 μg of streptomycin/ml. RF3 and ΔYC cells were maintained in the same medium containing 1 mg of Geneticin (G418)/ml. CHO-infection medium was Ham F-12 containing 30 mM $MgCl_2$ and 2% FCS, without Geneticin. Cells were grown at 37°C, and infection was carried out at 34°C under a 5% CO_2 atmosphere.

Virus. HRV2 was originally obtained from the American Type Culture Collection. An HRV2 variant adapted to replicate in CHO cells was isolated by blind passages alternating between HeLa and CHO-RF3 cells. Cells in a 162-cm^2 flask were challenged with virus at 10 50% tissue culture infective doses ($TCID_{50}$)/cell at 34°C for 30 min, medium with nonbound virus was replaced by fresh infection medium, and cells were incubated for 24 h to allow for infection. Virus eventually produced in the CHO cells was liberated by three consecutive freeze-thaw cycles, and HeLa cells were infected with the lysates. Whereas initially no cytopathic effect (CPE) was seen in the CHO cells, HeLa cells were usually lysed after 24 h. However, after 12 cycles CPE appeared in the CHO cells and persisted even upon CHO to CHO passaging for more than five times. The variant population, termed $HRV2_{CHO}$, replicated in both CHO cell lines but with different kinetics (see below).

Radiolabeling of HRV2. HeLa cells were grown in a 162-cm^2 flask until ca. 80% confluent, washed twice with phosphate-buffered saline (PBS), and incubated with 20 ml of methionine-cysteine-free Dulbecco modified Eagle medium supplemented with 2% dialyzed FCS, 100 U of penicillin/ml, 100 μg of streptomycin/ml, 2 mM L-glutamine, and 30 mM $MgCl_2$ for 4 h at 37°C. The medium was replaced by fresh methionine-cysteine-free medium, and virus was added at 1,000 $TCID_{50}$/cell. The cells were incubated for 4 h at 34°C to allow for viral internalization and host cell shutoff. Portions (15 ml) of the old medium were replaced by fresh infection medium containing 2% dialyzed FCS. After the addition of 1 mCi of [^{35}S]methionine-cysteine (Hartmann Analytic GmbH, Braunschweig, Germany), incubation was continued for 16 h. Cells were broken by three cycles of freezing-thawing, and debris was removed by centrifugation at 20,000 rpm (Ty65 rotor) for 20 min at 4°C. Virus was pelleted at 50,000 rpm (Ty65 rotor) for 2 h and suspended in 1 ml of HBBS supplemented with 2% FCS overnight at 4°C. Insoluble material was removed by centrifugation in a benchtop centrifuge. Remaining free radiolabel was removed by pelleting two times in a Beckman Optima TLX benchtop ultracentrifuge (TLA 100.3 rotor) at 70,000 rpm for 1 h. The viral pellet was finally resuspended in 200 μl of HBBS–2% FCS and stored at 4°C. Incorporated radioactivity was quantified by liquid scintillation counting (Tricarb; Packard, Meriden, CT); only radiochemically pure virus preparations (i.e., only viral proteins visible in the autoradiogram), as checked on a reducing 15% sodium dodecyl sulfate-polyacrylamide gel, were used. To ensure the absence of subviral particles, the preparations were stored over *S. aureus*-2G2 immunocomplexes that were removed by centrifugation before using the virus. The monoclonal antibody (MAb) 2G2 specifically recognizes subviral particles (31).

FACS quantification of LDLR expression. CHO cells were detached from 162-cm^2 culture flasks by incubation in 5 ml of 10 mM EDTA in PBS at 37°C for 5 min. The cells were washed with PBS and resuspended in Ham F-12 growth medium to allow for resaturation of cell surface LDLRs with Ca^{2+} at 37°C for 30 min. After two washes in ice-cold HBBS, the cells were resuspended in ice-cold fluorescence-activated cell sorting (FACS) buffer (HBBS supplemented with 2% FCS) at $\sim 2 \times 10^6$ cells/ml, followed by incubation under slow rotation for 1 h at 4°C. The cells were dispensed in 2-ml Eppendorf tubes at $\sim 2 \times 10^6$ cells/sample, pelleted at 1,000 × *g* for 5 min, resuspended in 200 μl of FACS buffer containing chicken immunoglobulin Y (IgY) directed against the ligand-binding domain of human LDLR (prepared by standard techniques) at 2.5 μg/ml. The cells were then incubated on ice for 1 h by gently shaking the tubes every other 10 min. After three washes with 1 ml of ice-cold HBBS, phycoerythrin-conjugated donkey anti-chicken secondary antibody (Jackson Immunoresearch) was added at 1:100 in 200 μl of FACS buffer. After 30 min of incubation, the cells were washed

twice with cold HBBS, resuspended in 1 ml of cold HBBS, transferred into 5-ml polypropylene FACS tubes, and kept on ice until analyzed. Cell-associated fluorescence corresponding to receptor expression was measured in a Becton Dickinson LSR-I flow cytometer, using the CellQuest Pro software for data analysis.

Quantification of cell attachment of HRV2. CHO cells expressing wt or truncated LDLR were grown in six-well plates until ca. 80% confluent. The growth medium was discarded, the cells were washed with ice-cold HBBS, 20,000 cpm of ^{35}S-labeled HRV2 in ice-cold infection medium was added per well, and the plates were incubated for 1 h at 4°C for virus binding. Unbound virus was removed by three washes with ice-cold HBBS, and the cells were lysed in 500 μl of RIPA buffer on ice for 15 min and transferred into scintillation vials. The wells were washed with 500 μl of RIPA buffer and with 500 μl of HBBS, the washes were combined with the cell lysates, and the cell-associated radioactivity was measured in a liquid scintillation counter (Tricarb).

Release of LDLR-bound HRV2 from CHO cells after low-pH treatment. CHO cells were grown in six-well plates until confluent. The medium was removed, and the cells were incubated in cold HBBS for 10 min at 4°C and challenged with 20,000 cpm of ^{35}S-labeled HRV2 in ice-cold CHO infection medium for 1 h at 4°C. Unbound virus was removed by washing the samples with ice-cold HBBS, and the cells were exposed to isotonic 30 mM MES buffers of pH 4.8 to 7.0 (with increments of 0.2 pH units) for 20 min at 4°C. Samples were reneutralized by the addition of the adequate volumes of 1 M Tris base. The virus released into the supernatant and remaining cell-associated virus were quantified separately by scintillation counting as described above. In a separate experiment, the effect of the duration of low-pH incubation and reneutralization on virus dissociation was determined. Cells were incubated at pH 5.0, 6.0, and 7.0 for 20, 45, and 90 min, followed by reneutralization to pH 7.0 for 0, 10, and 45 min.

Modeling endosomal virus conversion at the plasma membrane and influence of WIN-52084-2. The capsid-binding drug was dissolved at 0.5 mg/ml in 50% dimethyl sulfoxide. For each assay 30,000 cpm of ^{35}S-labeled HRV2 was preincubated in 20 μl of 150 mM NaCl (pH 7.5) containing WIN-52084-2 at a final concentration of 20 μg/ml for 30 min at room temperature. As a control, the virus was preincubated in the same solution without the WIN compound. Eventually, the non-native virus was removed by immunoprecipitation with MAb 2G2-*S. aureus* immunocomplexes prepared as follows. A 500-μl portion of fixed, heat-killed *S. aureus* cells from a 10% stock suspension was pelleted at 10,000 rpm for 1 min in a benchtop Eppendorf centrifuge. The pellet was washed twice with 1 ml of PBS and twice with 1 ml of RIPA buffer. Bacteria were resuspended in 400 μl of RIPA buffer, and 100 μl of rabbit HRV2-antiserum was added, followed by incubation for 1 h at room temperature. Bacteria were pelleted, washed three times with RIPA buffer, and finally resuspended in 500 μl of RIPA buffer containing 0.04% sodium azide. Since protein A binds rabbit IgG much better than mouse IgG, MAb 2G2 was bound via rabbit anti-mouse IgG by using the same procedure.

CHO cells were grown in six-well plates until confluent and preincubated in cold HBBS for 10 min at 4°C. After challenge with 20,000 cpm of ^{35}S-labeled HRV2 (untreated and preincubated with the antiviral, respectively) in CHO infection medium at 4°C for 1 h, unbound virus was removed, and the cells were further incubated in isotonic buffers of pH 4.8 to 7.0 for 20 min at 4°C as described above. The buffers were reneutralized, and the cells were further incubated for 20 min at 4°C to allow for virus release. Supernatants (1 ml) were collected in 2-ml Eppendorf tubes, the cells were washed twice with 250 μl of HBBS, the washes were combined with the supernatants, and 300 μl of 6× RIPA buffer was added. The cells were lysed in 500 μl of RIPA buffer on ice for 15 min and collected in 2-ml Eppendorf tubes. The wells were rinsed twice with 500 μl of RIPA buffer, and the washes were combined with the cell lysates. Debris was removed by centrifugation. Supernatants and cell lysates were processed separately for sequential immunoprecipitation. First, subviral particles were recovered by the addition of 20 μl of MAb 2G2-*S. aureus* immunocomplexes, followed by incubation for 2 h at room temperature. Bacteria were pelleted and washed twice with 200 μl of RIPA buffer. Remaining native virus in supernatants and washes was precipitated with 20 μl of rabbit HRV2 antibody-*S. aureus* immunocomplexes. Pellets were washed twice with 200 μl of RIPA buffer and scintillation counted. Conversion of native virus into subviral particles was calculated by dividing the sum of 2G2-precipitated counts by the total counts (i.e., the sum of 2G2 and anti-HRV2 precipitated counts). Conversion at pH 4.8 was set to 100% and conversion at pH 7.0 to 0%.

Kinetics of virus conversion. CHO cells were grown in six-well plates, preincubated in cold HBBS for 10 min at 4°C, and challenged with 20,000 cpm of ^{35}S-labeled HRV2 at 4°C for 1 h. Unbound virus was removed by extensive washing with ice-cold HBBS, and the cells were incubated in 1 ml of CHO infection medium at 34°C, allowing for virus internalization and uncoating. At the times given in the text, the cells were lysed without removing the incubation medium by adding 200 μl of 6× RIPA buffer. Cell debris was removed by centrifugation. To monitor the uncoating, subviral particles were immunoprecipitated with MAb 2G2, and the remaining native virus was immunoprecipitated with HRV2 antiserum, followed by quantification by liquid scintillation counting as described above, and the ratios of 2G2 precipitated counts over total counts were calculated.

Time-dependent colocalization of virus and LDLR. CHO cells were seeded onto 13-mm glass coverslips (Menzel, Braunschweig, Germany) and grown until 80% confluent. Cells were washed with PBS containing 1 mM $CaCl_2$ and 1 mM $MgCl_2$ (PBS^{++}), preincubated in 200 μl of CHO infection medium for 30 min at 37°C, cooled to 4°C, and challenged with HRV2 at 900 $TCID_{50}$/cell for 1 h. Unbound virus was removed by three washes with 2 ml of ice-cold PBS^{++}, and the cells were incubated in 500 μl of prewarmed CHO infection medium for 4, 20, and 60 min (chase). The coverslips were transferred into a six-well plate on ice and washed with 2 ml of ice-cold PBS^{++} for 5 min. The cells were fixed for 30 min with 300 μl of 4% paraformaldehyde in PBS^{++}, quenched with 300 μl of 50 mM NH_4Cl in PBS for 10 min, washed three times, and permeabilized with 300 μl of 0.2% Triton X-100 in PBS for 5 min. Nonspecific binding sites were blocked with 200 μl of 10% goat serum in PBS (Gibco/Invitrogen) for 30 min. All antibodies were diluted with PBS containing 10% goat serum. HRV2 was detected with MAb 8F5 (40) at 10 μg/ml, followed by Alexa 568-conjugated goat anti-mouse IgG (1:1,000; Molecular Probes, Eugene, OR), and LDLR was detected with chicken anti-human LDLR IgY (10 μg/ml) and Alexa 488-conjugated goat anti-chicken IgG (1:1,000; Molecular Probes). Cells were washed four times for 10 min each time with 5 ml of PBS, and nuclei were stained with DRAQ5 (Biostatus, Shepshed, Leicestershire, United Kingdom). Coverslips were briefly dipped in double-distilled H_2O and mounted in Mowiol. Cells were viewed with a Zeiss Axiovert 200 microscope (Carl Zeiss, Jena, Germany) equipped with an UltraView ERS laser confocal system (Perkin-Elmer, Shelton, CT). Twelve-bit images of highest resolution (1,344 × 1,024 pixels; no binning) were acquired through a 63×/1.4 Plan-Apochromat lens (Carl Zeiss). Images were taken with the same exposure time, and emission was discriminated by sequential acquisition. For Z-stack analysis, at least 15 images were recorded at 0.2-μm intervals with a piezo-driven Z stage. UltraView software was used to correct for background fluorescence and to determine the extent of colocalization.

Effect of HRV2 internalization on LDLR expression. RF3 and ΔYC cells were preincubated in serum-free Ham F-12 medium for 1 h at 34°C. HRV2 at 1,500 $TCID_{50}$/cell was internalized in serum-free Ham F-12 medium for 6 h. Cells were then cooled, washed, fixed, and permeabilized with methanol at −20°C for 10 min and processed for indirect immunofluorescence microscopy for the detection of LDLR (see above) and LAMP2 (anti-human CD107B mouse antibody 1:400; BD Biosciences/Pharmingen), followed by Alexa 488-conjugated goat anti-chicken IgG and Alexa 568-conjugated goat anti-mouse IgG, respectively. Nuclei were stained with Hoechst dye (1 μg/ml; for epifluorescence microscopy) and DRAQE5 (1:500; for confocal microscopy), and cells were embedded in Mowiol. LDLR expression and the extent of colocalization with LAMP2 was investigated by epifluorescence microscopy using a Zeiss Axioplan 2 fluorescence microscope equipped with a C-Apochromat 40× lens and Axiovision software. Confocal microscopy was carried out as described above.

Kinetics of the infection of CHO cells with $HRV2_{CHO}$. CHO cells grown in six-well plates were challenged with $HRV2_{CHO}$ at 10 $TCID_{50}$/cell at 4°C for 1 h. Unbound virus was removed by extensive washing with ice-cold HBBS, and the cells were incubated at 34°C in 2 ml of CHO infection medium. At time zero (to determine bound virus) and at 3, 6, 9, 12, 16, 22, 26, 31, and 36 h, the cells were subjected to three freeze-thaw cycles, cell debris was removed, and the virus titers were determined in HeLa cells.

RESULTS

At pH 5.3 LDLR releases LDL via intramolecular competition of its β-propeller domain for the ligand binding repeats L4 and L5 (5, 6, 37) or, as more recently suggested, via allosteric conformational changes (48). Since conversion of HRV2 into subviral particles during infection also occurs at similar pH values in late endosomes (16), structural changes of receptor and virus might take place concomitantly. Therefore, we sought to determine whether the β-propeller function was also important for minor group rhinovirus infection. Since human cells defective in expression of the receptors recognized by minor group HRVs are not available, all experiments were

carried out using CHO cells lacking endogenous LDLR as a consequence of a mutation (*ldla7* cells) (25). These cells were transfected to stably express human wt LDLR (RF3 cells) or a mutant receptor lacking the YWTD–β-propeller and the EGF-C domain (ΔYC cells).

Immunofluorescence microscopy and FACS analysis revealed that the expression levels of the LDLRs in the two cell lines were not identical (not shown). In particular, despite being grown in the presence of the selecting agent Geneticin, the concentration of wt LDLR was comparatively low in most of the cells. Therefore, both cell lines were subjected to FACS sorting, and cells expressing the respective receptors at similar levels were collected and expanded. This resulted in reasonably homogeneous populations; binding of radiolabeled HRV2 at 4°C was almost identical for both cell lines (ca. 70% ± 3.5% of total input virus) with low background binding (3.9% ± 0.7% related to the receptor-expressing cells) as determined for non-transfected CHO-*ldla7* control cells that lack functional LDLR. These cells were used for all experiments.

Structural changes and uncoating of HRV2 at the low endosomal pH can be mimicked at the plasma membrane by incubation of receptor-bound virus in acidic buffers (8). Since dissociation of the virus from its receptor when still in its native conformation might strongly decrease productive infection, we first investigated the possible role of the β-propeller domain in this process. The experiments were carried out with the two CHO cell lines by incubation of plasma membrane-bound virus in low-pH buffer. To avoid depletion of the Ca ions that are necessary to maintain the receptor in its native conformation, we used MES buffer instead of the acetate-phosphate buffers applied in the previous study (8).

HRV2 remains attached to CHO cells upon acidification unless reneutralized. ^{35}S-labeled HRV2 was bound to wt LDLR and mutant LDLR expressed on the respective CHO cell line for 1 h at 4°C. Unbound virus was washed away with ice-cold HBBS, and bound virus was exposed to a series of isotonic MES buffers of pH 4.8 to 7.0 for 20 min. In contrast to the previous results with HeLa cells (8), we found that the CHO cells did not release bound virus at any pH value, not even from the cells expressing wt LDLR on prolonged incubation at the lowest pH. This is most probably the result of the ~10-fold-higher LDLR expression level in the transfected cells than in HeLa cells. It suggests that HRV2 either remained receptor bound in its native form or had converted to subviral particles that were handed over to the cell membrane. However, substantial and rapid virus release was noticed after reneutralization to pH 7.0 (data not shown). The hydrophobic A-particles associate with liposomes (28), whereas the hydrophilic empty B-particles do not (24, 28). Therefore, these data imply that HRV2, when bound to CHO cells and exposed to low pH, dissociates from the cells uniquely upon reneutralization in the form of empty capsids.

LDLR binding stabilizes HRV2 against low pH-induced conversion. We next set out to identify the nature of the viral material remaining bound and being released. The experiment above was repeated, and subviral particles and native virus in the supernatant were determined by sequential immunoprecipitation with MAb 2G2 that specifically recognizes subviral particles (18, 31) and rabbit anti-HRV2 IgG. This method has been extensively used previously for quantification of the conversion of HRV2 into subviral particles (3, 19, 34). The same procedure was carried out with the cellular fraction after cell lysis with RIPA buffer. Immunoprecipitates were quantified by liquid scintillation counting (Fig. 1). Similar to the results with HeLa cells (8), the conformational alterations of HRV2 bound to CHO cells expressing wt LDLR occurred within a pH range from <6.0 to ~5.4, following a typical sigmoid curve. However, when virus was bound to β-propeller-negative LDLR, the curve was shifted toward lower pH values by ~0.3 pH units.

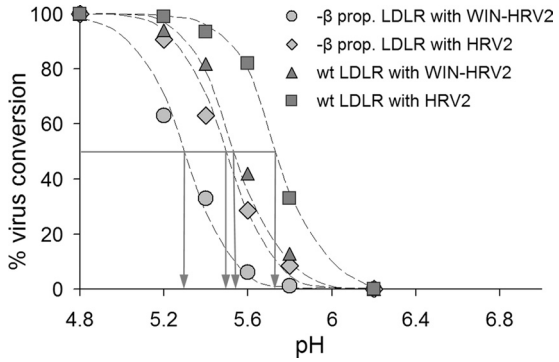

FIG. 1. Conversion of LDLR-bound HRV2 at the plasma membrane by incubation in isotonic buffers of different pH. Radiolabeled HRV2 either untreated or preincubated with the antiviral capsid-binder WIN-52084 was attached to the cells at 4°C for 1 h, unbound virus was removed, and the cells were incubated at 4°C for 20 min in isotonic buffers with the pH values indicated. The buffers were reneutralized by adding Tris base, and the cells were further incubated for 20 min to allow for virus release. Converted virus was immunoprecipitated with MAb 2G2 and remaining native virus with anti-HRV2 antiserum from both the supernatants and cell lysates. Total conversion at pH 4.8 was set to 100%, and no conversion at pH 7.0 was set to 0%. Note that the propeller-negative LDLR stabilizes the virus against its conversion to a similar extent as the antiviral substance; the two different types of protection effects were additive.

Capsid-binding drugs, such as I(S), also named WIN-52084 (from the Sterling Winthrop company that originally manufactured them), displace fatty acids naturally present in the hydrophobic pocket of the capsid and protect HRVs against low pH-induced conversion into subviral A-particles (16, 21). Therefore, the same experiment was carried out with HRV2 that had been preincubated with this drug. Stabilization by the compound also resulted in a shift of the conversion curve of wt LDLR-bound HRV2 toward lower pH values. This increase in stability at low pH was almost identical to that caused by truncated LDLR. Apparently, in the absence of the β-propeller domain the high-avidity attachment of the receptor via several ligand-binding modules stabilizes the native conformation of the virus. This is in line with earlier data of Nicodemou et al. (32), who demonstrated stabilization of HRV2 by the soluble concatemeric pentamer of module 3 (V33333) of VLDLR in vitro. Stabilization by WIN-52084 and the β-propeller negative receptor were additive, shifting the sigmoid curve even more toward lower pH values (Fig. 1). Under our experimental conditions virtually no virus was released from the cells upon acidification. However, upon reneutralization, a large percentage was found in the cell supernatant, and 80 to 100% of it was in the form of subviral particles at any pH value for all four experimental conditions (data not shown).

Upon endocytosis in HeLa cells, HRV2 is shuttled from

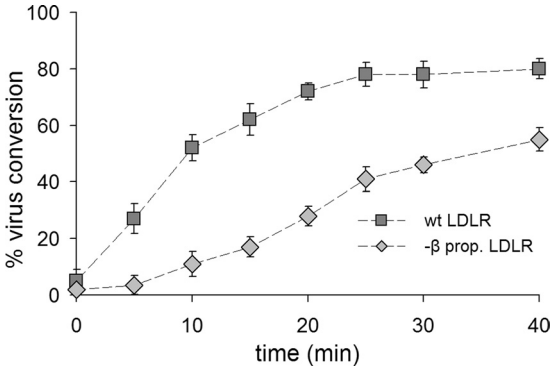

FIG. 2. Viral conversion is delayed and reduced in CHO cells expressing the β-propeller-negative LDLR compared to wt LDLR. Radiolabeled HRV2 was attached to cells grown in six-well plates at 4°C for 1 h, unbound virus was washed away, and the cells were incubated in 1 ml of infection medium at 34°C, allowing for virus internalization and uncoating. At the time points indicated, the cells were lysed without removing the incubation medium. Converted virus was immunoprecipitated with MAb 2G2 and remaining native virus was immunoprecipitated with anti-HRV2 antiserum and scintillation counted. The percentage of virus conversion was calculated as 2G2-precipitated counts divided by total precipitated counts and set to 0% at time zero. Note the delay and lower extent of uncoating when the virus enters via the truncated receptor. Error bars indicate the means ± the standard deviations (SD) ($n = 3$).

early to late endosomes within endosomal carrier vesicles (ECV). The RNA is released from the virus either in ECV or in late endosomes (4), and the remaining empty capsids move on to lysosomes, where they are degraded. Therefore, productive RNA release must happen within a window of opportunity in the correct compartment. The experiments mimicking the situation in endosomes at the plasma membrane suggest that the β-propeller might facilitate virus conversion at comparatively higher pH values at earlier times. Thereby, the time window for RNA release would be longer, which could influence the efficiency of infection. Therefore, we investigated viral conformational changes during cell entry.

Conversion of native HRV2 to subviral particles is delayed when internalized via β-propeller-deficient LDLR. Radiolabeled HRV2 was attached to the cells at 4°C for 1 h, unbound virus was washed away with cold HBBS, and the cells were incubated in infection medium at 34°C to allow for virus internalization and conversion in endosomes. At various times, the cells were lysed by adding RIPA buffer without removing the incubation medium. Subviral particles and remaining native virus were recovered by sequential immunoprecipitation with MAb 2G2 and anti-HRV2 antiserum and determined by liquid scintillation counting. The percentage of virus conversion was calculated as the ratio of 2G2-precipitated counts over total precipitated counts and set to 0% at time zero. As seen in Fig. 2, virus conversion was strongly delayed and reduced when entry occurred via the truncated receptor.

The dissociation of HRV2 from the two forms of LDLR within endosomes was also assessed via the time-dependent colocalization of HRV2 and LDLR by confocal immunofluorescence microscopy. HRV2 was bound to the plasma membrane of CHO cells expressing the respective receptor on ice, and the cells were further incubated at 34°C for the times

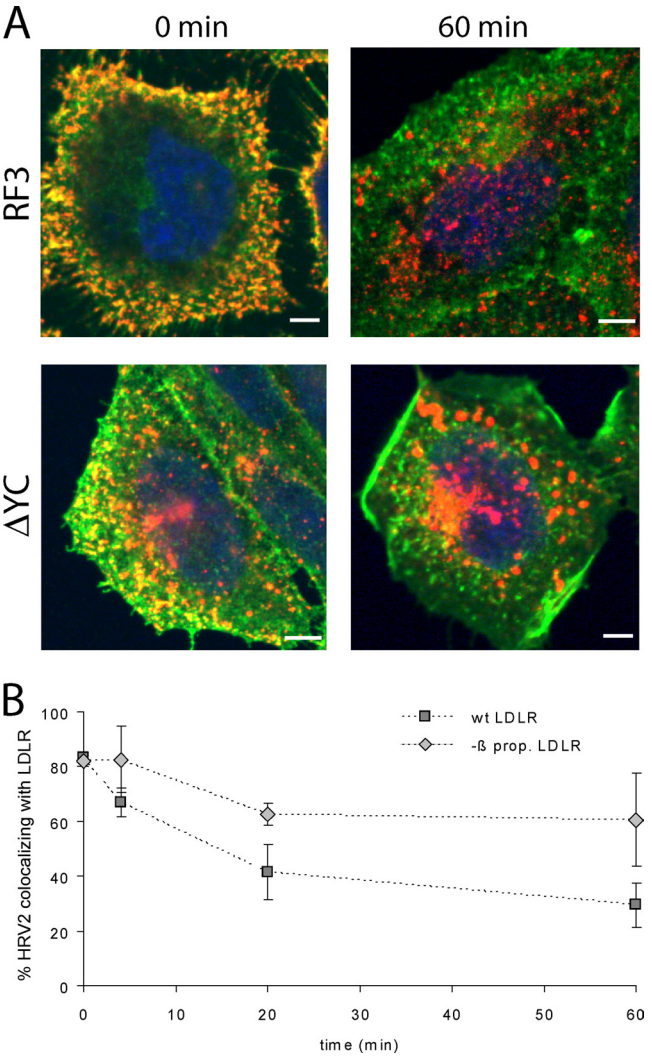

FIG. 3. HRV2 dissociation from LDLR is delayed when the β-propeller is deleted. HRV2 was bound at 4°C to CHO cells grown on coverslips, and entry was initiated by adding warm medium. At the times indicated, the cells were fixed and permeabilized, and LDLR and HRV2 were detected by specific antibodies, followed by Alexa 488-conjugated goat anti-mouse IgG and Alexa 568-conjugated goat anti-chicken IgG, respectively. (A) Representative fluorescent images of one focal plane through the perinuclear region are shown after HRV2 binding (0 min) and 60 min after warming to 34°C. LDLR, green; HRV2, red. (B) The percent colocalization of virus and receptor was calculated from immunofluorescence microscopy images as in panel A. Colocalization at time zero was set to 100%. Error bars indicate the means ± the SD ($n = 3$).

indicated in Fig. 3. Virus and receptor were differentially labeled with suitable specific antibodies and visualized (Fig. 3A). Colocalization was determined by using UltraView software (Fig. 3B). In agreement with virus-receptor dissociation in early endosomes (8), colocalization of HRV2 and receptor rapidly decreased in time. Furthermore, when the virus entered via the β-propeller-negative receptor, this dissociation occurred at a substantially slower rate and only to a minor extent.

Infection is delayed when HRV2 is internalized via β-propeller-deficient LDLR. Most HRVs fail to replicate in nonhu-

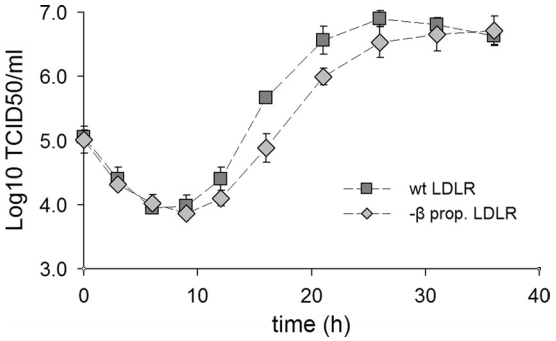

FIG. 4. Infection kinetics of CHO cell-adapted HRV2 in cells expressing wt and β-propeller-negative LDLR. Cells seeded in six-well plates were challenged with $HRV2_{CHO}$ at 10 $TCID_{50}$/cell at 4°C for 1 h. After the removal of unbound virus, the cells were incubated at 34°C. At the times indicated, the cells were broken by three cycles of freeze-thawing, and the virus titer was determined. Note the significant delay in virus production in the cells expressing the truncated receptor. Error bars indicate means ± the SD ($n = 3$).

man cells, and challenge of the CHO cell lines with HRV2 did not result in productive infection. However, adaptation of HRV2 to mouse L cells has been reported (47). The variants showed mutations within nonstructural viral proteins, indicating that receptor binding was not affected. We thus used the same strategy for adapting HRV2 to replicate in hamster cells. After 12 blind passages alternating between RF3-CHO cells and HeLa cells, a population of HRV2 variants, termed $HRV2_{CHO}$, was selected that caused CPE and multiplied in both CHO lines. Figure 4 depicts the infection kinetics of $HRV2_{CHO}$ in the two lines. The virus titer decreased at the early times after challenge, indicating uncoating of incoming virus. From about 9 h onward, replication was evident with the virus titer attaining a plateau after about 30 h. The most obvious difference between the two cell lines is seen between 12 and 26 h; the cells expressing the wt receptor produced up to 6 times more virus at 16 h postinfection, with a difference of ~5 h in reaching the plateau.

HRV2 directs the β-propeller-deficient LDLR to lysosomes. Deletion of the entire EGFP-homology domain of LDLR has been shown to inhibit dissociation of bound LDL, impairs receptor recycling, and results in lysosomal degradation of the receptor-ligand complex (10). Since the β-propeller is the main player in the conformational changes at low pH (5, 37), we thought it likely that the ΔYC deletion mutant used in our experiments behaves identically. To assess whether HRV2 internalization results in degradation of the mutant LDLR, we studied colocalization of LDLR with the lysosomal marker LAMP2 by fluorescence microscopy. CHO cells expressing wt or β-propeller-negative LDLR were grown on coverslips and incubated for 30 min in serum-free medium, and HRV2 at 1,500 $TCID_{50}$/cell was continuously internalized for 6 h at 34°C. The cells were chilled, washed, fixed, permeabilized, and incubated with mouse anti-LAMP2 antibody, followed by Alexa 568-conjugated goat anti-mouse IgG. LDLRs were revealed with chicken anti-LDLR IgY, followed by Alexa 488-conjugated goat anti-chicken IgG. For control purposes, mock-infected cells were incubated under the same conditions. Internalization of HRV2 into RF3 cells had no significant

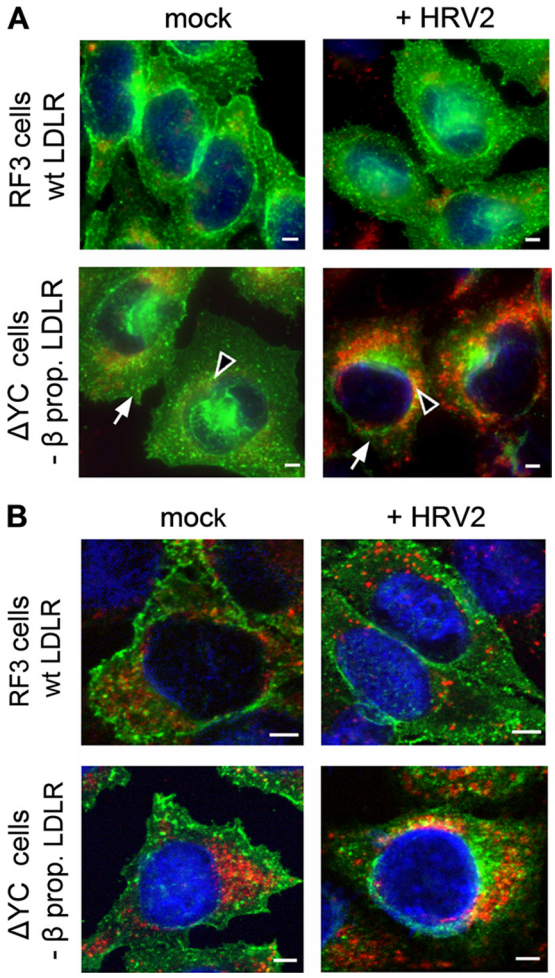

FIG. 5. Continuous HRV2 internalization leads to degradation of mutant but not wt LDLR. RF3 and ΔYC cells were preincubated in serum-free Ham F-12 medium, and HRV2 at 1,500 $TCID_{50}$/cell was internalized for 6 h. Cells were cooled, washed, and processed for indirect immunofluorescence microscopy for the detection of LDLR (green) and LAMP2 (red). Nuclei were stained with Hoechst dye (for epifluorescence) and DRAQE5 (for confocal microscopy). (A) Conventional epifluorescence microscopy. All images were taken with the same exposure time in the respective channel and identical settings were used for illustration with the Axiovision software. Overlay images are shown. Arrowheads indicate perinuclear and arrows indicate plasma membrane localization of the receptors. (B) Confocal images were taken by using the same laser power and exposure time in the respective channel. Multicolor images shown were obtained with identical gray level settings in each channel. Of 20 sections through the cells, the focal plane through the nucleus is depicted. Bar, 2 μm.

influence on the total fluorescence and thus on the concentration of wt LDLR (Fig. 5A, upper panels). Furthermore, little colocalization of LDLR with the late endosome/lysosome marker LAMP2 was seen in the absence and in the presence of HRV2 (Fig. 5B, upper panels). In contrast, in ΔYC cells HRV2 uptake resulted in decreased LDLR levels mainly at the plasma membrane (arrows) but not in the perinuclear area (Fig. 5A, lower panels, arrowheads). The decrease in plasma membrane localization of the mutant receptors appears to be due to their lysosomal degradation as deduced from the higher extent of colocalization of receptors with LAMP2 (Fig. 5B,

lower panels). Collectively, this indicates that the virus directs the truncated receptor to lysosomes.

DISCUSSION

LDL has been shown to dissociate from plasma membrane LDLR at pH <5.5 (10); if the entire EGFP-domain or the β-propeller together with the EGF-C domain is absent from the receptor, LDL release is reduced to 10% compared to 100% for wt LDLR (6, 7). The 3D X-ray structure of LDLR determined at pH 5.3 revealed an intramolecular interaction between modules LA4 and LA5 and the β-propeller and thereby nicely explained the underlying mechanism at the molecular level (37). In the present study we took advantage of CHO-*ldla7* cells that are deficient in the endogenous receptor but had been stably transfected to overexpress human wt LDLR (RF3 cells) and LDLR lacking the β-propeller, together with the EGF-C domain (ΔYC cells). We demonstrated that the β-propeller domain is not only important for the LDL metabolism but also exerts a similar function in the conversion and release of minor group HRVs, exemplified by HRV2. LDLR is thus not only a vehicle for virus delivery, but it also fine-tunes the location and timeliness of RNA transfer into the cytosol. By comparing cells expressing either wt LDLR (RF3) or LDLR whose β-propeller was deleted (ΔYC cells), it became clear that, in the absence of this latter domain, HRV2 was less readily released from the receptor and the structural changes associated with uncoating and required for RNA release were only observed at a lower pH. The final conversion to 80S particles appears to be facilitated by reneutralization. We are currently investigating whether this could also occur in vivo via pores in the endosomal membrane, allowing for the exit of protons. We also compared the two forms of the receptor with respect to infection and virus production. Since HRV2 fails to replicate in rodent cells, it was adapted to grow in these cells by a series of blind passages alternating between RF3 and HeLa cells. The resultant HRV2 variant (termed $HRV2_{CHO}$) grew to roughly one-fifth of the titer attained in HeLa cells. It was previously shown that adaptation to mouse cells by a similar protocol does not modify the viral capsid but rather introduces mutations into nonstructural proteins (17, 27). Therefore, it is highly unlikely that receptor interaction is modified in this variant, and it was legitimate to use it for our analyses. As a consequence of β-propeller deletion, the infection was delayed and less efficient. Stabilization of HRV2 by a receptor construct carrying five copies of V3, the third module of VLDLR arranged in tandem, has been noted earlier (32). This effect is most probably due to the strong multivalent attachment of the receptor modules around the fivefold axes of icosahedral symmetry (36). It appears that even LDLR, in which only repeats 1, 2, 4, and 5 possess the tryptophan essential for virus binding (45), exhibits sufficient avidity for protecting the virus against conformational changes at low pH.

Conversion of the virus to subviral particles in endosomes and viral de novo synthesis were delayed in ΔYC cells compared to RF3 cells. These data indicate that wt LDLR facilitates viral conformational modification and subsequent steps such as virus release from the receptor, RNA uncoating, and RNA transfer into the cytoplasm. This is brought about by the β-propeller that supposedly competes with the virus for ligand-binding repeats LA4 and LA5. Our data correlate well with the results for LDL release mentioned above; only ca. 15% of HRV2 was released from the mutated receptor in ΔYC cells and 70% of HRV2 was released from the wt receptor in RF3 cells after 60 min internalization.

Endocytosed ligands are transported through the endocytic pathway to lysosomes and thereby become exposed to an increasingly lower pH; pH 6.5 to 6.0 in early endosomes, pH 5.5 to 5.0 in late endosomes, and pH 4.5 to 4.0 in lysosomes. Sorting of LDL from transferrin, a marker of the recycling pathway, occurs in early (sorting) endosomes within 2 to 4 min (12, 15, 30). However, the low-pH structure of LDLR was analyzed at pH 5.3 (5, 6, 37). This raises the question of which additional factors may aid ligand release in early endosomes. Since binding of ligands to the LDLR family is Ca^{2+} dependent (9), a mildly acidic pH and a low endosomal Ca ion concentration could cooperatively facilitate ligand dissociation as shown in in vitro experiments (1). Since the V-ATPase is electrogenic, inward proton transport has to be balanced by inward chloride and/or outward cation (K^+, Na^+, and Ca^{2+}) movement. Indeed, upon pinching-off the plasma membrane, endocytic vesicles rapidly alter their internal milieu from one corresponding to the extracellular environment (pH neutral and high concentrations of chloride, sodium, and calcium ions) to an acidic pH. Although the endosomal chloride concentration is lowered to ~17 mM within 3 min, it subsequently increases to 60 mM as the pH decreases to 5.3 along the lysosomal pathway (42). In contrast, a continuous decrease in endosomal Ca^{2+} was observed; its concentration dropped within 3 min to 29 μM and to ~3 μM after 20 min (14). Indeed, various calcium channels (e.g., a "transient receptor potential-like Ca-channel" [38]) and various mucolipin calcium channels (29) were identified in endosomal subcompartments that exhibit distinct properties and therefore may contribute to low endosomal calcium as well as to endosomal pH regulation.

Lack of ligand dissociation from LDLR affects receptor trafficking. For β-VLDL, the EGFP domain had no influence on binding, internalization, and degradation, but the mutant LDLRs failed to recycle. This resulted in a time-dependent loss of mutant receptors, presumably due to their lysosomal degradation (10). Taken together, the failure to dissociate ligand from LDLR results in receptor trafficking to lysosomes (2). This is in line with our results that demonstrate that HRV2 directs the mutant receptor to lysosomes.

Based on the earlier finding that virus is released from its receptor in the native state at the pH prevailing in early endosomes (8), we rather expected that propeller-deficient LDLR would increase the efficiency of infection by holding the virus close to the endosomal membrane until conversion occurs. In contrast, our conversion assays showed that the virus was not released at any pH values, unless the incubation buffers were reneutralized. These results do not necessarily contradict previous data on HeLa cells (8), where release of native HRV2 at pH 6.0 was shown, for the following reasons. (i) HeLa cells express, in addition to LDLR, LRP and VLDLR. Infection of HeLa cells is inhibited to 80 to 90% by receptor-associated protein (M. Brabec et al., unpublished results), which is indicative for a preferential role of LRP1 and/or VLDLR in HRV2 entry. (ii) Intracellular trafficking of HRV2 bound to LRP1 may be distinct from LDLR. (iii) The low-pH

buffers used by Brabec et al. contained phosphate but lacked calcium and thus facilitated release of native virus (see above). Whether the virus dissociates from the receptor when still in its native state or just upon conversion most probably depends on the interrelation of multiple factors, such as the avidity of virus-receptor binding and the pH range of virus conversion compared to that of the receptor switch.

Taken together, our results underscore the role of the β-propeller in LDLR for minor group HRV infection. LDLR is thus not just a simple vehicle for delivery of the virus into endosomes but is also a well-chosen carrier combining high-avidity multimodule binding with an intrinsic release mechanism. If the release mechanism is impaired, the virus fails to undergo conversion at the correct time, and the correct intracellular compartment and infection is less efficient.

ACKNOWLEDGMENTS

We thank Stephen Blacklow for the gift of the recombinant CHO cells and Irene Goesler for virus production.

This study was supported by the Austrian Science Foundation (FWF) grant P17516-B10.

REFERENCES

1. **Arias-Moreno, X., A. Velazquez-Campoy, J. C. Rodriguez, M. Pocovi, and J. Sancho.** 2008. Mechanism of low density lipoprotein (LDL) release in the endosome: implications of the stability and Ca^{2+} affinity of the fifth binding module of the LDL receptor. J. Biol. Chem. **283:**22670–22679.
2. **Basu, S. K., J. L. Goldstein, R. G. Anderson, and M. S. Brown.** 1981. Monensin interrupts the recycling of low density lipoprotein receptors in human fibroblasts. Cell **24:**493–502.
3. **Bayer, N., D. Schober, M. Huttinger, D. Blaas, and R. Fuchs.** 2001. Inhibition of clathrin-dependent endocytosis has multiple effects on human rhinovirus serotype 2 cell entry. J. Biol. Chem. **276:**3952–3962.
4. **Bayer, N., D. Schober, E. Prchla, R. F. Murphy, D. Blaas, and R. Fuchs.** 1998. Effect of bafilomycin A1 and nocodazole on endocytic transport in HeLa cells: implications for viral uncoating and infection. J. Virol. **72:**9645–9655.
5. **Beglova, N., H. Jeon, C. Fisher, and S. C. Blacklow.** 2004. Cooperation between fixed and low pH-inducible interfaces controls lipoprotein release by the LDL receptor. Mol. Cell **16:**281–292.
6. **Beglova, N., H. Jeon, C. Fisher, and S. C. Blacklow.** 2004. Structural features of the low-density lipoprotein receptor facilitating ligand binding and release. Biochem. Soc. Trans. **32:**721–723.
7. **Boswell, E. J., H. Jeon, S. C. Blacklow, and A. K. Downing.** 2004. Global defects in the expression and function of the low density lipoprotein receptor (LDLR) associated with two familial hypercholesterolemia mutations resulting in misfolding of the LDLR epidermal growth factor-AB pair. J. Biol. Chem. **279:**30611–30621.
8. **Brabec, M., G. Baravalle, D. Blaas, and R. Fuchs.** 2003. Conformational changes, plasma membrane penetration, and infection by human rhinovirus type 2: role of receptors and low pH. J. Virol. **77:**5370–5377.
9. **Brown, M. S., J. Herz, and J. L. Goldstein.** 1997. LDL receptor structure: calcium cages, acid baths and recycling receptors. Nature **388:**629–630.
10. **Davis, C. G., J. L. Goldstein, T. C. Sudhof, R. G. Anderson, D. W. Russell, and M. S. Brown.** 1987. Acid-dependent ligand dissociation and recycling of LDL receptor mediated by growth factor homology region. Nature **326:**760–765.
11. **Davis, M. P., G. Bottley, L. P. Beales, R. A. Killington, D. J. Rowlands, and T. J. Tuthill.** 2008. Recombinant VP4 of human rhinovirus induces permeability in model membranes. J. Virol. **82:**4169–4174.
12. **Dunn, K. W., and F. R. Maxfield.** 1992. Delivery of ligands from sorting endosomes to late endosomes occurs by maturation of sorting endosomes. J. Cell Biol. **117:**301–310.
13. **Fisher, C., N. Beglova, and S. C. Blacklow.** 2006. Structure of an LDLR-RAP complex reveals a general mode for ligand recognition by lipoprotein receptors. Mol. Cell **22:**277–283.
14. **Gerasimenko, J. V., A. V. Tepikin, O. H. Petersen, and O. V. Gerasimenko.** 1998. Calcium uptake via endocytosis with rapid release from acidifying endosomes. Curr. Biol. **8:**1335–1338.
15. **Ghosh, R. N., D. L. Gelman, and F. R. Maxfield.** 1994. Quantification of low density lipoprotein and transferrin endocytic sorting HEp2 cells using confocal microscopy. J. Cell Sci. **107:**2177–2189.
16. **Gruenberger, M., D. Pevear, G. D. Diana, E. Kuechler, and D. Blaas.** 1991. Stabilization of human rhinovirus serotype-2 against pH-induced conformational change by antiviral compounds. J. Gen. Virol. **72:**431–433.
17. **Harris, J. R., and V. R. Racaniello.** 2005. Amino acid changes in proteins 2B and 3A mediate rhinovirus type 39 growth in mouse cells. J. Virol. **79:**5363–5373.
18. **Hewat, E. A., and D. Blaas.** 2006. Nonneutralizing human rhinovirus serotype 2-specific monoclonal antibody 2G2 attaches to the region that undergoes the most dramatic changes upon release of the viral RNA. J. Virol. **80:**12398–12401.
19. **Huber, M., M. Brabec, N. Bayer, D. Blaas, and R. Fuchs.** 2001. Elevated endosomal pH in HeLa cells overexpressing mutant dynamin can affect infection by pH-sensitive viruses. Traffic **2:**727–736.
20. **Khan, A. G., J. Pichler, A. Rosemann, and D. Blaas.** 2007. Human rhinovirus type 54 infection via heparan sulfate is less efficient and strictly dependent on low endosomal pH. J. Virol. **81:**4625–4632.
21. **Kim, S., T. J. Smith, M. S. Chapman, M. G. Rossmann, D. C. Pevear, F. J. Dutko, P. J. Felock, G. D. Diana, and M. A. McKinlay.** 1989. Crystal structure of human rhinovirus serotype-1A (Hrv1A). J. Mol. Biol. **210:**91–111.
22. **Kingsley, D. M., and M. Krieger.** 1984. Receptor-mediated endocytosis of low density lipoprotein: somatic cell mutants define multiple genes required for expression of surface-receptor activity. Proc. Natl. Acad. Sci. USA **81:**5454–5458.
23. **Kistler, A., P. C. Avila, S. Rouskin, D. Wang, T. Ward, S. Yagi, D. Schnurr, D. Ganem, J. L. Derisi, and H. A. Boushey.** 2007. Pan-viral screening of respiratory tract infections in adults with and without asthma reveals unexpected human coronavirus and human rhinovirus diversity. J. Infect. Dis. **196:**817–825.
24. **Korant, B. D., K. Lonberg Holm, J. Noble, and J. T. Stasny.** 1972. Naturally occurring and artificially produced components of three rhinoviruses. Virology **48:**71–86.
25. **Krieger, M., M. S. Brown, and J. L. Goldstein.** 1981. Isolation of Chinese hamster cell mutants defective in the receptor-mediated endocytosis of low density lipoprotein. J. Mol. Biol. **150:**167–184.
26. **Lee, W. M., S. S. Monroe, and R. R. Rueckert.** 1993. Role of maturation cleavage in infectivity of picornaviruses: activation of an infectosome. J. Virol. **67:**2110–2122.
27. **Lomax, N. B., and F. H. Yin.** 1989. Evidence for the role of the P2 protein of human rhinovirus in its host range change. J. Virol. **63:**2396–2399.
28. **Lonberg Holm, K., L. B. Gosser, and E. J. Shimshick.** 1976. Interaction of liposomes with subviral particles of poliovirus type 2 and rhinovirus type 2. J. Virol. **19:**746–749.
29. **Martina, J. A., B. Lelouvier, and R. Puertollano.** 2009. The calcium channel mucolipin-3 is a novel regulator of trafficking along the endosomal pathway. Traffic **10:**1143–1156.
30. **Mayor, S., J. F. Presley, and F. R. Maxfield.** 1993. Sorting of membrane components from endosomes and subsequent recycling to the cell surface occurs by a bulk flow process. J. Cell Biol. **121:**1257–1269.
31. **Neubauer, C., L. Frasel, E. Kuechler, and D. Blaas.** 1987. Mechanism of entry of human rhinovirus 2 into HeLa cells. Virology **158:**255–258.
32. **Nicodemou, A., M. Petsch, T. Konecsni, L. Kremser, E. Kenndler, J. M. Casasnovas, and D. Blaas.** 2005. Rhinovirus-stabilizing activity of artificial VLDL-receptor variants defines a new mechanism for virus neutralization by soluble receptors. FEBS Lett. **579:**5507–5511.
33. **Nurani, G., B. Lindqvist, and J. M. Casasnovas.** 2003. Receptor priming of major group human rhinoviruses for uncoating and entry at mild low-pH environments. J. Virol. **77:**11985–11991.
34. **Prchla, E., E. Kuechler, D. Blaas, and R. Fuchs.** 1994. Uncoating of human rhinovirus serotype 2 from late endosomes. J. Virol. **68:**3713–3723.
35. **Prchla, E., C. Plank, E. Wagner, D. Blaas, and R. Fuchs.** 1995. Virus-mediated release of endosomal content in vitro: different behavior of adenovirus and rhinovirus serotype 2. J. Cell Biol. **131:**111–123.
36. **Querol-Audi, J., T. Konecsni, J. Pous, O. Carugo, I. Fita, N. Verdaguer, and D. Blaas.** 2009. Minor group human rhinovirus-receptor interactions: geometry of multimodular attachment and basis of recognition. FEBS Lett. **583:**235–240.
37. **Rudenko, G., L. Henry, K. Henderson, K. Ichtchenko, M. S. Brown, J. L. Goldstein, and J. Deisenhofer.** 2002. Structure of the LDL receptor extracellular domain at endosomal pH. Science **298:**2353–2358.
38. **Saito, M., P. I. Hanson, and P. Schlesinger.** 2007. Luminal chloride-dependent activation of endosome calcium channels: patch clamp study of enlarged endosomes. J. Biol. Chem. **282:**27327–27333.
39. **Schober, D., P. Kronenberger, E. Prchla, D. Blaas, and R. Fuchs.** 1998. Major and minor-receptor group human rhinoviruses penetrate from endosomes by different mechanisms. J. Virol. **72:**1354–1364.
40. **Skern, T., C. Neubauer, L. Frasel, P. Gruendler, W. Sommergruber, W. Zorn, E. Kuechler, and D. Blaas.** 1987. A neutralizing epitope on human rhinovirus type 2 includes amino acid residues between 153 and 164 of virus capsid protein VP2. J. Gen. Virol. **68:**315–323.
41. **Snyers, L., H. Zwickl, and D. Blaas.** 2003. Human rhinovirus type 2 is internalized by clathrin-mediated endocytosis. J. Virol. **77:**5360–5369.
42. **Sonawane, N. D., and A. S. Verkman.** 2003. Determinants of [Cl−] in recycling and late endosomes and Golgi complex measured using fluorescent ligands. J. Cell Biol. **160:**1129–1138.

43. **Tyrrell, D. A. J., and R. M. Chanock.** 1963. Rhinoviruses: a description. Science **141:**152–153.
44. **Uncapher, C. R., C. M. Dewitt, and R. J. Colonno.** 1991. The major and minor group receptor families contain all but one human rhinovirus serotype. Virology **180:**814–817.
45. **Verdaguer, N., I. Fita, M. Reithmayer, R. Moser, and D. Blaas.** 2004. X-ray structure of a minor group human rhinovirus bound to a fragment of its cellular receptor protein. Nat. Struct. Mol. Biol. **11:**429–434.
46. **Vlasak, M., M. Roivainen, M. Reithmayer, I. Goesler, P. Laine, L. Snyers, T. Hovi, and D. Blaas.** 2005. The minor receptor group of human rhinovirus (HRV) includes HRV23 and HRV25, but the presence of a lysine in the VP1 HI loop is not sufficient for receptor binding. J. Virol. **79:**7389–7395.
47. **Yin, F. H., and N. B. Lomax.** 1983. Host range mutants of human rhinovirus in which nonstructural proteins are altered. J. Virol. **48:**410–418.
48. **Zhao, Z., and P. Michaely.** 2008. The epidermal growth factor homology domain of the LDL receptor drives lipoprotein release through an allosteric mechanism involving H190, H562, and H586. J. Biol. Chem. **283:**26528–26537.